Z. Phys. C – Particles and Fields 48, 433–444 (1990)

Zeitschrift für Physik C Particles and Fields

Measurement of the asymmetry of b quark production in e^+e^- annihilation at $\sqrt{s}=35$ GeV

TASSO Collaboration

W. Braunschweig, R. Gerhards, F.J. Kirschfink[1], H.-U. Martyn

I. Physikalisches Institut der RWTH Aachen, Federal Republic of Germany[a]

H.M. Fischer, H. Hartmann, J. Hartmann, E. Hilger, A. Jocksch[2], R. Wedemeyer

Physikalisches Institut der Universität Bonn, Federal Republic of Germany[a]

B. Foster, A.J. Martin[3]

H.H. Wills Physics Laboratory, University of Bristol, Bristol, UK[b]

E. Bernardi[4], J. Chwastowski[5], A. Eskreys[5], K. Genser[6], H. Hultschig, P. Joos, H. Kowalski, A. Ladage, B. Löhr, D. Lüke, P. Mättig[15], D. Notz, J.M. Pawlak[6], K.-U. Pösnecker, E. Ros, D. Trines, R. Walczak[6], G. Wolf

Deutsches Elektronen-Synchrotron DESY, Hamburg, Federal Republic of Germany

H. Kolanoski

Institut für Physik, Universität Dortmund, Federal Republic of Germany[a]

J. Krüger, E. Lohrmann, G. Poelz, W. Zeuner[7]

II. Institut für Experimentalphysik der Universität Hamburg, Federal Republic of Germany[a]

D. Binnie, J. Hassard, J. Shulman[8], D. Su[9], I. Tomalin, A. Watson

Department of Physics, Imperial College, London, UK[b]

F. Barreiro, G. Cases, L. Hervas, J. del Peso[g]

Universidad Autonoma de Madrid, Madrid, Spain[c]

M.G. Bowler, P.N. Burrows[10], R.J. Cashmore, M.E. Veitch

Department of Nuclear Physics, Oxford University, Oxford, UK[b]

J.C. Hart, D.H. Saxon

Rutherford Appleton Laboratory, Chilton, Didcot, UK[b]

S. Brandt, M. Holder

Fachbereich Physik der Universität-Gesamthochschule Siegen, Federal Republic of Germany[a]

Y. Eisenberg, U. Karshon, A. Montag, D. Revel, E. Ronat[11], N. Wainer

Weizmann Institute, Rehovot, Israel[d]

A. Caldwell[12], D. Muller[13], S. Ritz[12], D. Strom[14], M. Takashima[7], Sau Lan Wu, G. Zobernig

Department of Physics, University of Wisconsin, Madison, WI, USA[e]

Received 25 May 1990

[1] Now at Lufthansa, Hamburg, FRG
[2] Now at Fa. Fichtner, Stuttgart, FRG
[3] Now at Queen Mary Westfield College, London
[4] Now at Robert Bosch GmbH, Schwieberdingen, FRG
[5] Now at Inst. of Nuclear Physics, Cracow, Poland
[6] Now at Warsaw University[f], Poland
[7] Now at CERN, Geneva, Switzerland
[8] Now at University College, London, UK
[9] Now at Rutherford Appleton Laboratory, Chilton, Didcot, UK
[10] Now at MIT, Cambridge, MA, USA
[11] deceased
[12] Now at Columbia University, NY, USA
[13] Now at SLAC, Stanford, CA, USA
[14] Now at University of Chicago, Chicago, IL, USA
[15] Heisenberg fellow, now at CERN, Geneva, Switzerland

[a] Supported by Bundesministerium für Forschung und Technologie
[b] Supported by UK Science and Engineering Research Council
[c] Supported by CAICYT
[d] Supported by the Minerva Gesellschaft für Forschung GmbH
[e] Supported by US Dept. of Energy, contract DE-AC02-76ER000881 and by US Nat. Sci. Foundation Grant number INT-8313994 for travel
[f] Partially supported by grant CPBP 01.06
[g] Supported by DAAD

Abstract. The forward-backward asymmetry in the reaction $e^+e^- \to b\bar{b}$ has been determined at centre of mass energies near 35 GeV using the TASSO detector. We report results from three different methods. The combined result of the measurements is $\overline{A_b} = -0.21 \pm 0.08$ ignoring $B^0\bar{B}^0$ mixing. Taking mixing into account leads to a corrected asymmetry of $\overline{A_b^{\text{cor}}} = -0.28 \pm 0.11$. The axial vector coupling constant of the b quark as calculated from the corrected asymmetry is $a_b = -1.2 \pm 0.5$ to be compared with the value $a_b^{\text{SM}} = -1$ from the standard model.

1 Introduction

There is a forward backward asymmetry in the reaction $e^+e^- \to q\bar{q}$ originating from the interference between photon and Z^0 exchange. In the standard model the asymmetry for charge $-1/3$ quarks is predicted to be large, $A_q \simeq -0.23$ for b quarks at 35 GeV centre of mass energy including higher order QED and QCD corrections. In order to determine the b asymmetry it is necessary to identify $b\bar{b}$ events and, within the events, the direction of the b quark. The event jet axis provides a good measure of the line of flight of the quark but it is also necessary to distinguish the quark direction from that of the antiquark.

In studies of the forward-backward asymmetry in $c\bar{c}$, the distinctive properties of D^* decay have been used to identify the quark direction. In $b\bar{b}$ events the charge of high transverse momentum leptons has been used to distinguish b from $\bar{b}$, but there are few significant measurements of the asymmetry in $b\bar{b}$ events (Table 1).

In this paper we present results for b asymmetry extracted by three different methods. One is obtained from a study of inclusive electron production, one from high transverse momentum muon production. In both these methods lepton charge is used to tag the quark charge. In the third method a sample of b enriched events is used. Enrichment was accomplished by using the long b lifetime, and the sign of the quark is determined by the weighted jet charge.

Table 1. The measured b quark asymmetries [32]

Experiment	Method	$\sqrt{s}$[GeV]	A_b
TPC	e	29.0	-0.34 ± 0.33
TPC	μ	29.0	-0.15 ± 0.20
MAC	μ	29.0	0.034 ± 0.070
CELLO	e, μ	35.0	-0.222 ± 0.081
CELLO	e, μ	43.0	-0.491 ± 0.165
JADE	μ	34.6	-0.228 ± 0.065
JADE	e, μ	35.0	-0.116 ± 0.048
MARK J	μ	37.0	-0.21 ± 0.19
PLUTO	μ	34.8	-0.36 ± 0.25
AMY	μ	55.2	-0.72 ± 0.28
TASSO (1984)	μ	34.5	-0.375 ± 0.275
TASSO (1984)	e	34.6	-0.25 ± 0.22
This paper	e, μ, jet	35.0	-0.21 ± 0.08

2 The asymmetry from inclusive electrons

In this method the primary quark charge is measured via the electrons from the semileptonic decays of the b quarks. The different flavours were separated using the transverse momentum of the prompt electron and an event shape quantity.

The data were collected with the TASSO detector at the PETRA storage ring at DESY, from February 1980 to July 1982 and from March to November 1986. A total of 52584 multihadronic events with centre of mass energies between 33 GeV and 36 GeV and with an integrated luminosity of 168.3 pb^{-1} were selected using the TASSO standard criteria [1].

2.1 Event selection

The TASSO detector has been described in detail elsewhere [2] and here we simply note that the information used was taken from the drift chamber with a momentum resolution of

$$\frac{\sigma_p}{p} = 0.016 \cdot \sqrt{1.0 + p^2} \qquad p \text{ in GeV/c} \tag{1}$$

and from the lead liquid argon shower counters located above and below the TASSO magnet coil.

Because the electron identification is essential for this analysis and mainly done with the help of the shower counters they are briefly described. The active surface area of the shower counters covers approximately 40% of the solid angle. This is reduced to 35% because particles which lie within 5 cm of the edge of the active area are not accepted. The shower counters consist of a system of towers and strips. The towers are composed of lead plates with a front surface area of $7.1 \times 7.1\ \text{cm}^2$ (front towers) and $14.2 \times 14.2\ \text{cm}^2$ (back towers) and a thickness of 2 mm. They are stacked so as to point to the interaction region. Four front towers are followed by one back tower. The towers provide a measurement of the total energy of electromagnetic showers with a resolution determined from electrons with an energy between $1.0\ \text{GeV} < E < 5.0\ \text{GeV}$ [3] of

$$\frac{\sigma_E}{E} = \frac{0.136}{\sqrt{E}} + 0.03 \qquad E \text{ in GeV.} \tag{2}$$

The strips are 2 cm wide and plated onto copper clad epoxy circuit boards. They run orthogonal to the beam axis (φ strips) and parallel to it (z strips). The strips provide a position resolution determined from electrons with energy $1.0\ \text{GeV} < E < 5.0\ \text{GeV}$ [3] of

$$\sigma_\varphi = \left(\frac{0.77}{p} + 0.53\right) \text{cm} \qquad p \text{ in GeV/c,} \tag{3}$$

$$\sigma_z = \left(\frac{0.48}{p} + 1.27\right) \text{cm} \qquad p \text{ in GeV/c.} \tag{4}$$

These errors contain the multiple scattering error, the error on the position measurement of the shower and the error on the extrapolated track position.

Electrons are identified using the information of the drift chamber and the shower counters. The energy deposition in the shower counters as well as the longitudinal and lateral distributions of the shower energy were required to be compatible with those of an electron of the observed momentum. The most important requirements were [4]:

1. The momentum of the track was required to be at least 1.0 GeV/c.
2. The track was required to be not identified as a converted photon.
3. The shower was required to be assigned to exactly one track.
4. The momentum of the charged track was required to agree with the total shower energy measured in the front and back towers.
5. The extrapolated position of the track was required to agree with the position of the shower as measured in the strips.
6. The shower energy measured in the front towers (E_F) and in the back towers (E_B) was required to satisfy:

$$\frac{E_B}{E_F} < 0.8 + 0.1 \cdot p \qquad p \text{ in GeV/c.} \tag{5}$$

7. The lateral distribution of the shower energy measured in the strips was required to be consistent with an electron shower.

With these cuts a total of 918 events with at least one identified electron was selected from the multihadronic sample. Those inclusive electron events have an average centre of mass energy of 34.8 GeV. Most of these events have exactly one electron ($\simeq 99\%$). Detailed Monte Carlo studies indicate that the tracks identified as electrons are mainly prompt electrons from semileptonic decays of b or c quarks, converted photons and hadrons misidentified as electrons. The contribution from the decay of π or K mesons or from faked tracks is negligible.

2.2 Simulation

To compare the results with predictions of the electroweak theory, we need an estimation of effects introduced by the event acceptance and investigation of the background. In this analysis Monte Carlo events were used, generated using the following schemes:

HOYER: The partons were generated according to first order QCD [5] including initial state radiative effects [6]. The fragmentation model used the independent jet fragmentation idea of Field and Feynman [7]. The strong coupling constant α_s was set to 0.19, the transverse momentum parameter of the quarks was $\sigma_q = 0.35$ GeV/c and the fraction of pseudoscalars among the mesons produced in the fragmentation was 0.42. The parameter a_f of the fragmentation function was set to 0.56 [8]. The response of the detector is simulated in great detail using EGS [9] for the simulation of electromagnetic showers in the liquid argon calorimeters. The shower development of hadrons in the calorimeters has also been simulated, using the method of [10].

QCDFF: The partons were generated according to first order electroweak theory using the extended FKSS scheme (neglecting the asymmetry) including initial state radiation [6] and to second order QCD. The parameters used were the same as for the HOYER model with the exception of α_s which was set to 0.155. The fragmentation model used the Peterson fragmentation function [11] for b and c quarks ($\varepsilon_b = 0.01$ and $\varepsilon_c = 0.075$). These events were only passed through the inner detector.

LUND: The partons were generated according to first order electroweak theory including initial state radiation [6] and to second order QCD. The fragmentation model used the LUND string fragmentation [12] with the symmetric fragmentation function ($a = 0.96$ and $b = 0.70\,\text{GeV}^{-2}$) for all flavours. These events were only passed through the inner detector.

The above parameters had been tuned to give good agreement between the simulation results and the TASSO data [13].

The Hoyer Monte Carlo, providing a full calorimeter simulation, was used to determine the electron identification and detection efficiency. The QCDFF and LUND generators were used for modelling the data and to extract an estimate of the systematic errors of the Monte Carlo simulation.

2.3 Flavour separation

To measure the asymmetry one has to distinguish between the different reactions which lead to a track identified as coming from an electron. We distinguish between events with prompt electrons and events with identified electrons from other sources. Prompt electrons come from original b quark production ($b \to e$), from original c quark production ($c \to e$) and from events in which a b quark has subsequently decayed to a c quark which then produced an observable electron ($b \to c \to e$). The background events may have an original b quark ($b \to X$), an original c quark ($c \to X$) or an u, d or s quark ($uds \to X$). In cases with more than one identified electron we used only the electron with the largest transverse momentum with respect to the sphericity axis.

To distinguish between these six types of events we used the transverse momentum p_t of the electron with respect to the sphericity axis and an event shape quantity called transverse mass M_t first introduced by Marshall [14].

$$M_t = \frac{\sqrt{s}}{\sum_{i=1}^{N_t} E_i} \cdot \sum_{i=1}^{N_t} |p_i^{\perp}| \qquad i \neq i_e \tag{6}$$

where E_i and $p_i^{\perp}$ are the energy and transverse momentum of particle i with respect to the event plane and

the sum runs over all N_t charged tracks except the electron.

The event axis and the event plane are calculated with the sphericity tensor which on average reproduces the original quark direction to within 8° [15]. Because tracks with high transverse momenta (as tends to be the case for prompt electrons) may lead to much bigger deviations with respect to the quark direction, the tensor in this analysis is calculated only from tracks which were not identified as an electron.

Probability distributions for all six types of events were determined from the Monte Carlo simulation. We used QCDFF and LUND Monte Carlo events (see Sect. 2.2). To simulate the electron identification, the efficiency to identify a track which points to the calorimeter was determined with the HOYER Monte Carlo. The efficiencies as a function of the momentum were determined for prompt electrons, converted photons and for hadrons.

The probability distributions were smoothed by fitting a phenomenological function $h(M_t, p_t)$ to them. Details of this procedure can be found in [4]. The resulting (normalized) probability density functions are $\rho(M_t, p_t)$. To measure the separation between the six event types one can define a matrix T_{ij} [14].

$$T_{ij}=\frac{1}{N_i}\cdot\frac{1}{N_j}\int_0^\infty\int_0^\infty h_i(M_t, p_t)\,h_j(M_t, p_t)\,dM_t\,dp_t \tag{7}$$

with

$$N_i^2=\int_0^\infty\int_0^\infty h_i^2(M_t,p_t)\,dM_t\,dp_t$$

and

$$i=be, bce, ce, bX, cX, udsX.$$

For identical distributions we then have $T_{ij}=1$, whereas if the distributions are completely separated we have $T_{ij}=0$. The elements of the matrix as determined from the Monte Carlo are given in Table 2. It can be seen that events of the type $b\to e$ are well separated from other processes, whereas the separation among the other five types of events is difficult.

We used the probability distribution functions to determine the number of prompt electrons N_p in our data sample, performing a maximum likelihood fit to all events.

Table 2. Fractions for all sorts of reactions contributing to the inclusive electron sample

T_{ij}	$b\to e$	$b\to c\to e$	$c\to e$	$b\to x$	$c\to x$	$uds\to x$
$b\to e$	1	0.69	0.53	0.56	0.46	0.45
$b\to c\to e$		1	0.90	0.95	0.85	0.81
$c\to e$			1	0.86	0.94	0.94
$b\to x$				1	0.90	0.85
$c\to x$					1	0.99
$uds\to x$						1

Table 3. The fractions of the six types of processes giving rise to electron candidates

Process	Fraction f_i
$b\to e$	18.9±1.5%
$b\to c\to e$	7.7±0.6%
$c\to e$	30.6±2.4%
$b\to x$	3.0±0.3%
$c\to x$	16.5±1.7%
$uds\to x$	23.3±2.4%

$$\ln L=\sum_{i=1}^{N}\ln\left(\frac{d^2N}{dM_t\,dp_t}\right) \tag{8}$$

with

$$\begin{aligned}\frac{d^2N}{dM_t\,dp_t}=&N_p\cdot f_p^{be}\cdot\rho_{be}(M_t, p_t)\\&+N_p\cdot f_p^{bce}\cdot\rho_{bce}(M_t, p_t)\\&+N_p\cdot f_p^{ce}\cdot\rho_{ce}(M_t, p_t)\\&+(N-N_p)\cdot f_x^{bX}\cdot\rho_{bX}(M_t, p_t)\\&+(N-N_p)\cdot f_x^{cX}\cdot\rho_{cX}(M_t, p_t)\\&+(N-N_p)\cdot f_x^{udsX}\cdot\rho_{udsX}(M_t, p_t)\end{aligned}$$

where f_p^i are the fractions of events with prompt electrons and f_x^i are the fractions of background events determined from the HOYER Monte Carlo (see Sect. 2.2). The result of the one parameter fit was:

$$N_p=525\pm41 \tag{9}$$

from 918 candidate events, which leads to the numbers and fractions shown in Table 3. To compare the Monte Carlo expectations with the data, one dimensional distributions in p_t and M_t were calculated from the two dimensional probability distribution functions by integrating over M_t and p_t respectively and weighted with the numbers determined above. As shown in Figs. 1 and 2 the agreement is very good.

The data can be split into a forward ($\cos\theta>0$) and a backward ($\cos\theta<0$) sample where $\cos\theta$ is calculated from (10) with q_e = charge of the prompt electron or positron candidate. δ = angle between prompt lepton candidate and sphericity axis, and $\theta_s<\pi/2$ angle between sphericity axis and incident electron (see Fig. 3).

$$\cos\theta=-\frac{q_e\cdot\cos\vartheta}{|q_e\cdot\cos\vartheta|}\cdot|\cos\theta_s|. \tag{10}$$

The cross section in (8) may then be written as

$$\frac{d^2N}{dM_t\,dp_t}=\begin{cases}\dfrac{d^2N^F}{dM_t\,dp_t} & \text{if } \cos\theta>0\\[2ex] \dfrac{d^2N^B}{dM_t\,dp_t} & \text{if } \cos\theta<0\end{cases}$$

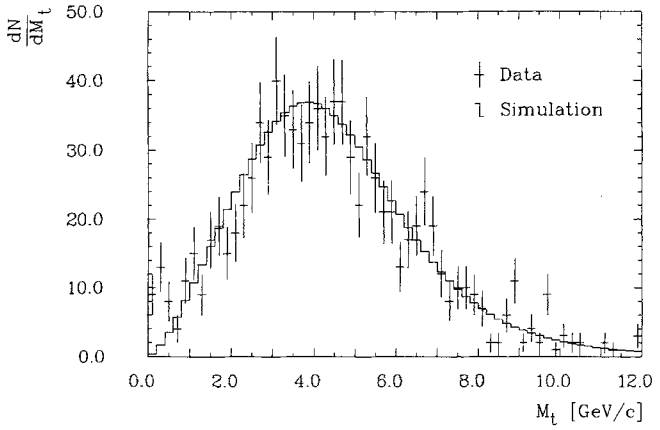

Fig. 1. Comparison of the M_t distributions with the Monte Carlo simulation

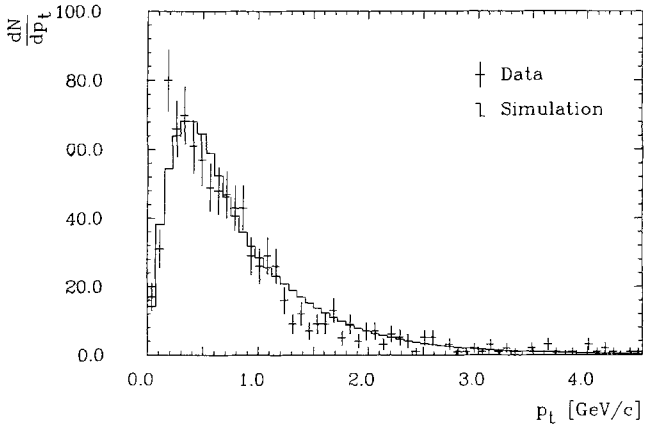

Fig. 2. Comparison of the p_t distributions with the Monte Carlo simulation

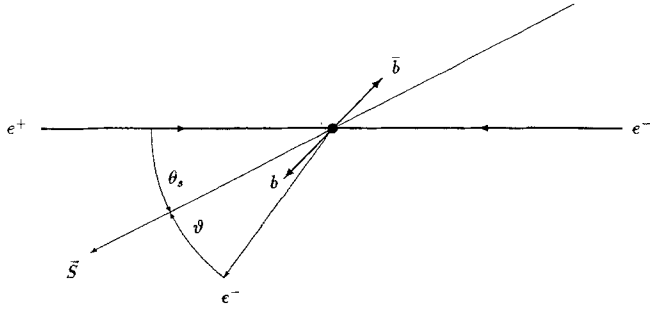

Fig. 3. Definition of the polar angle. The direction of the sphericity axis is labelled S

with

$$\frac{d^2N^{\mathrm{F}}}{dM_t\,dp_t} = N_b^{\mathrm{F}}\cdot f_b^{be}\cdot\rho_{be}(M_t,p_t) + N_b^{\mathrm{B}}\cdot f_b^{bce}\cdot f_{cas}^{+}\cdot\rho_{bce}(M_t,p_t) + N_b^{\mathrm{F}}\cdot f_b^{bce}\cdot f_{cas}^{-}\cdot\rho_{bce}(M_t,p_t) + N_c^{\mathrm{F}}\cdot\rho_{ce}(M_t,p_t) + (N^{\mathrm{F}}-N_{\mathrm{p}}^{\mathrm{F}})\cdot f_x^{bX}\cdot\rho_{bX}(M_t,p_t) + (N^{\mathrm{F}}-N_{\mathrm{p}}^{\mathrm{F}})\cdot f_x^{cX}\cdot\rho_{cX}(M_t,p_t) + (N^{\mathrm{F}}-N_{\mathrm{p}}^{\mathrm{F}})\cdot f_x^{udsX}\cdot\rho_{udsX}(M_t,p_t)$$

and the corresponding quantity $\dfrac{d^2N^{\mathrm{B}}}{dM_t\,dp_t}$, which has the indices F and B interchanged and where

$$N_{\mathrm{p}}^{\mathrm{F}} = N_b^{\mathrm{F}}\cdot f_b^{be} + N_b^{\mathrm{B}}\cdot f_b^{bce}\cdot f_{cas}^{+} + N_b^{\mathrm{F}}\cdot f_b^{bce}\cdot f_{cas}^{-}$$
$$N_{\mathrm{p}}^{\mathrm{B}} = N_b^{\mathrm{B}}\cdot f_b^{be} + N_b^{\mathrm{F}}\cdot f_b^{bce}\cdot f_{cas}^{+} + N_b^{\mathrm{B}}\cdot f_b^{bce}\cdot f_{cas}^{-}$$
$$N_b^{\mathrm{B}} = (N^{\mathrm{F}}+N^{\mathrm{B}})\cdot f_b - N_b^{\mathrm{F}}$$
$$N_c^{\mathrm{B}} = (N^{\mathrm{F}}+N^{\mathrm{B}})\cdot f_c - N_c^{\mathrm{F}}$$

where N_b^{F}, N_b^{B}, N_c^{F} and N_c^{B} are the numbers of forward and backward events for b and c quarks respectively, f_b and f_c are the fractions of events with prompt electrons from b and c decay and f_b^{be} and f_b^{bce} are the fractions of b events from the process $b\to e$ and $b\to c\to e$. All these fractions are taken from Table 3. A complication comes from the events ($b\to c\to e$). A b quark in these events can lead to a positron or to an electron with a ratio of 6.5:1 [16], corresponding to the fractions $f_{cas}^{+}=0.87$ and $f_{cas}^{-}=0.13$.

To determine the numbers of forward events N_b^{F} and N_c^{F} a maximum likelihood fit similar to (8) was carried out. The result was

$$N_b^{\mathrm{F}} = 95\pm14 \Rightarrow N_b^{\mathrm{B}} = 149\pm24$$
$$N_c^{\mathrm{F}} = 132\pm19 \Rightarrow N_c^{\mathrm{B}} = 149\pm29 \qquad (11)$$

which leads to b and c quark asymmetries uncorrected for acceptance

$$A_b^{\mathrm{obs}} = -0.22\pm0.16 \quad\text{and}\quad A_c^{\mathrm{obs}} = -0.06\pm0.19. \qquad (12)$$

These numbers serve as a check for the general procedure, because the c quark asymmetry has been left as a free parameter. To check that the b asymmetry did not arise from a small region of the detector, the fit was also carried out in smaller angular intervals. The results are shown in Fig. 4. A forward-backward asymmetry of the correct sign is indicated.

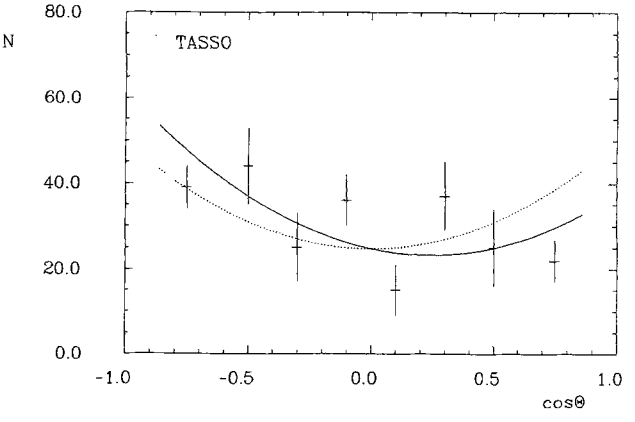

Fig. 4. The angular distribution of the $b\bar{b}$ events using the method of Sect. 2.3. The dotted curve shows the prediction of pure QED, the solid one is the standard model fit – uncorrected for acceptance

2.4 Results

To determine the asymmetry of the b quark a maximum likelihood fit was carried out to the whole data sample including the angular probability distribution function as follows.

$$\ln L = \sum_{i=1}^{N} \ln\left(\frac{1}{N}\cdot\frac{d^3N}{dM_t\,dp_t\,d(\cos\theta)}\right) \tag{13}$$

with

$$\begin{aligned}
&\frac{1}{N}\cdot\frac{d^3N}{dM_t\,dp_t\,d(\cos\theta)}\\
&= f_{be}\cdot\rho_{be}(M_t, p_t)\cdot[\tfrac{3}{8}(1+\cos^2\theta)+A_b\cos\theta]\\
&\quad+f_{bce}\cdot f^{+}_{cas}\cdot\rho_{bce}(M_t, p_t)\cdot[\tfrac{3}{8}(1+\cos^2\theta)-A_b\cos\theta]\\
&\quad+f_{bce}\cdot f^{-}_{cas}\cdot\rho_{bce}(M_t, p_t)\cdot[\tfrac{3}{8}(1+\cos^2\theta)+A_b\cos\theta]\\
&\quad+f_{bX}\cdot\rho_{bX}(M_t, p_t)\cdot[\tfrac{3}{8}(1+\cos^2\theta)]\\
&\quad+f_{ce}\cdot\rho_{ce}(M_t, p_t)\cdot[\tfrac{3}{8}(1+\cos^2\theta)-A_c\cos\theta]\\
&\quad+f_{cX}\cdot\rho_{cX}(M_t, p_t)\cdot[\tfrac{3}{8}(1+\cos^2\theta)]\\
&\quad+f_{udsX}\cdot\rho_{udsX}(M_t, p_t)\cdot[\tfrac{3}{8}(1+\cos^2\theta)]
\end{aligned}$$

where f and ρ are the fractions and the two-dimensional probability distribution functions. We checked that radiative corrections change this form insignificantly in comparison to the size of the errors. For the asymmetry of the c quark we use the averaged results of the measurements near 35 GeV given in Table 4. Using a value of $A_c = -0.151$ the fit which now does not depend on acceptance [17] leads to:

$$A_b(e) = -0.20 \pm 0.11 \pm 0.04 \tag{14}$$

where the first error is statistical and the second systematic. The systematic uncertainties were estimated by changing the fractions, the cascade fractions and the asymmetry of the c quark within their errors, leading to uncertainties of 0.02, 0.005 and 0.02 respectively. The uncertainty due to the calculation of the angle θ was estimated to be less than 0.01. The uncertainty coming from the simulation was set to 0.02. Thus the systematic error is approximately 0.02. The result (14) depends on the value of A_c, which is now fairly well measured (Table 4); its error is included in the systematic error. The unconstrained result (12) is consistent with (14).

Table 4. The measured c quark asymmetries near 35 GeV [33]

Experiment	$\sqrt{s}$ [GeV]	A_c
HRS	29.0	-0.099 ± 0.027
CELLO	35.0	-0.129 ± 0.088
JADE	35.0	-0.149 ± 0.067
MARK J	35.3	-0.160 ± 0.090
PLUTO	34.8	-0.16 ± 0.16
TASSO	35.8	-0.160 ± 0.043

3 The asymmetry from inclusive muons

The b asymmetry can also be determined by the selection of events containing a muon with high transverse momentum, because more than half of the muons from b decay have transverse momentum relative to the thrust axis $p_t > 1$ GeV/c. In TASSO, muon candidates are identified by hits in proportional wire chambers placed behind iron absorbers and covering 0.43 of 4π steradians. Prompt muons originate in b and c decay and there is background from decays of pions and kaons before the iron absorbers and from hadronic punch-through. A detailed account of the TASSO muon detectors and the simulation of background may be found in [18] together with a detailed comparison of data, at a mean energy of 34.5 GeV, with the results of Monte Carlo simulations.

In order to determine an asymmetry, events containing a muon candidate with high transverse momentum are divided into two jets with a plane normal to the thrust axis. A positive high transverse momentum muon in a jet tags that jet as likely to contain a $\bar{b}$; a negative muon serves as a b tag. In a previous paper [18] we carried out such an analysis. The forward-backward asymmetry was

$$A^{\text{obs}}(\mu_1) = -0.087 \pm 0.071. \tag{15}$$

After correction for geometrical acceptance, background due to punchthrough and the contribution of $c \to X\mu\nu$ the true forward-backward asymmetry for particles containing b quarks, over the full solid angle, was found to be

$$A_b(\mu_1) = -0.375 \pm 0.275 \tag{16}$$

at a mean centre of mass energy of 34.5 GeV.

We have now analysed an independent sample of data, corresponding to an integrated luminosity of $110\,\text{pb}^{-1}$, at a centre of mass energy of 35 GeV. The sample consists of 245 events which contain a good muon candidate with $p > 2$ GeV/c and $p_t > 1$ GeV/c, the magnitude of the cosine of the angle between the thrust axis and the beams being less than 0.8. There are 116 events with forward jets and 129 with backward jets, in the sense defined above, the observed forward-backward asymmetry of these 245 events being

$$A^{\text{obs}}(\mu_2) = -0.053 \pm 0.064. \tag{17}$$

Monte Carlo studies, using the same simulation of background as in [18], lead us to expect that these 245 events represent $82\,b \to \mu$, $15\,b \to c \to \mu$, $49\,c \to \mu$ and 99 background events. The observed forward-backward asymmetry is then

$$A^{\text{obs}}(\mu_2) = \frac{(82-15)\cdot A_b^{\text{obs}}(\mu_2) - 49\cdot A_c}{245} \tag{18}$$

assuming that the background is symmetrically distributed. The charm asymmetry A_c is expected to be -0.13

for the range of angles accepted, yielding a b quark asymmetry for the accepted range of

$$A_b^{\text{obs}}(\mu_2) = -0.29 \pm 0.24 \pm 0.07. \quad (19)$$

The first error is statistical, the second systematic; it takes into account the uncertainties of the c-quark asymmetry A_c, of the b semileptonic branching ratio and of the background.

Statistical errors in the Monte Carlo study are negligible in comparison with the statistical errors on the observed asymmetry. After correcting for the restricted angular range, we obtain for the b quark asymmetry defined over the full solid angle

$$A_b(\mu_2) = -0.33 \pm 0.27 \pm 0.08. \quad (20)$$

If this results is combined with the statistically independent result from [18] we obtain a b quark asymmetry determined using high transverse momentum muons of

$$A_b(\mu) = -0.35 \pm 0.19 \pm 0.08 \quad (21)$$

at an average centre of mass energy of 35 GeV.

4 The asymmetry from quark charge measurement

4.1 b Enrichment by lifetime

In order to select the b events from the hadronic sample a novel technique based on secondary vertex detection has been used. The technique exploits the relatively long lifetime of B hadrons. A similar method has been used previously for b tagging [19]. This analysis differs however in some important technical aspects, and will therefore be presented in some detail.

In order to reconstruct a B hadron decay vertex very good tracking precision is required. The vertex detector (VXD) [20] is therefore central to the analysis. Consequently only the data collected at 35 GeV after installation of the VXD have been used. These amount to 31176 hadronic events selected by our standard hadronic cuts. The spatial resolution of the VXD for hadronic tracks in this period has been found to be $\sim 110\,\mu$m, varying by $\pm 30\%$ depending on the VXD layer and hit position in the cell. After track-finding the tracks have been refitted in the plane perpendicular to the beams ($r-\phi$ plane) [23], allowing for multiple scattering between the VXD and the main drift chamber. The track impact parameter resolution achieved was $\sim 100\,\mu$m for high momentum tracks.

The tagging method itself depends on locating independently the production point (event vertex) and the decay vertex in a jet and comparing their positions. If a decay vertex is found significantly displaced from the production point, the jet is considered to be a b tag. Due to worse detector resolution in the z direction (along the beam) all the position measurements are performed in the $r-\phi$ plane only.

4.1.1 Production point finding. The starting point for the event vertex finding was the beam spot centre, determined on a run-by-run basis. Due to the relatively large beam size in the horizontal (x) direction, an attempt has been made to locate the production point for each event more precisely inside the beam profile. The method used was essentially the same as described in our previous publication [19].

4.1.2 Event and track selection. The events were selected from the standard hadronic sample requiring in addition that the VXD was on, and the beam spot was well reconstructed. 30520 events have been thus selected.

For each event the sphericity axis was determined, using tracks selected by our standard track quality criteria [1]. However for the vertex finding tracks found by the FELIX [22] trackfinder were used. All tracks have been refitted in two dimensions [23]. Cuts on momentum ($p > 0.6$ GeV/c), on the quality of the fit and on the distance of closest approach to the beam were applied [21]. The purpose of these cuts was to remove tracks from K^0 or Λ decays, photon conversions, tracks strongly affected by multiple scattering in the detector material, and tracks which were poorly reconstructed due to lack of hits or track finding mistakes. On average 5.2 tracks per event survived these cuts.

After selection the surviving tracks were assigned to jets. A jet was defined as a collection of tracks within a cone of 50° around the sphericity axis, on one side. In the following vertex finding procedure each jet was considered separately.

4.1.3 Vertex fitting. The next step was to look for a vertex in each jet. A vertex fit was performed by repeating the track fit for a set of tracks simultaneously, constraining the tracks to intersect at a common point. This condition gives an additional constraint in a two-dimensional fit only if at least three tracks are fitted. Therefore only combinations of three or more tracks were considered and the vertex fit was attempted only for jets with at least three tracks.

The vertex finding algorithm started with forming various combinations of available tracks. Each such combination was subjected to the following cuts:

1. $|\Sigma q_i| \leqq 3$, q_i is the charge of i-th track of the combination,
2. $\max \phi_{ij} > 0.3$ rad, ϕ_{ij} is the angle between the projections of tracks on the $r-\phi$ plane,
3. $\min \phi_{ij} > 0.02$ rad,
4. $\max \varphi_{ij} > 0.4$ rad, φ_{ij} is the angle between tracks measured in three dimensions.

The first cut was intended to remove combinations which, due to a large charge imbalance, are unlikely to come from a B hadron decay. Cuts 2 and 4 removed candidates with small opening angle. Due to the high mass of the b quark it is expected that its decay products will have relatively large opening angles, so the cut should not remove too many b decay candidates. On the other hand a vertex found from tracks very close

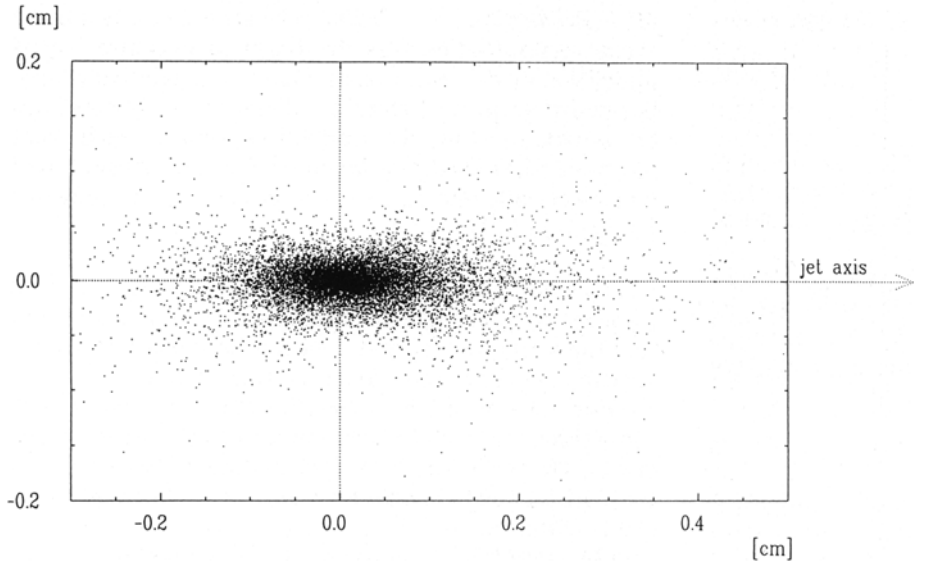

Fig. 5. Positions of the jet vertices found in 1986 data with respect to the interaction point. The picture shows 14402 points, 19 points are beyond the left margin of the frame, 39 beyond the right margin

to each other would have poorly determined position along the flight direction, and would therefore have small chance of being well separated from the production point. Finally, cut 3 removed combinations having a pair of very close tracks.

Each combination which fulfilled the above criteria was then passed to the fit program [23]. The combination was considered a vertex candidate if it passed the following cuts:

1. The vertex fit was successful in less than 10 iterations,
2. $\chi^2/\mathrm{NDF} < 1.3$ in the vertex fit,
3. $\Delta\chi^2$, the difference of χ^2 between the vertex fit and unconstrained track fits imply agreement at a confidence level $\mathrm{CL}(\Delta\chi^2, n-2) > 0.05$.

The quantity $\Delta\chi^2$ calculated for n tracks of common origin is expected to have a χ^2 distribution with $n-2$ degrees of freedom. The cut on confidence level associated with $\Delta\chi^2$ was therefore intended to remove vertices fitted to non-intersecting tracks. The other two cuts assured that the overall fit quality was good. Of all the found vertex candidates in a given jet, the one with best overall fit quality was kept as a jet vertex.

The above procedure applied to the data yielded 14460 jet vertices. Figure 5 shows the positions of 14402 of these vertices in a reference frame with the production point at (0,0) and the jet axis pointing in positive x direction. The majority of vertices are found to occupy an elliptical region of the approximate size 500 μm × 150 μm centered on the production point. This corresponds nicely to the average size of the vertex error ellipse returned by the vertex fitter (430 μm × 100 μm) folded with the interaction point finding error.

A careful examination of Fig. 5 reveals that the distribution is slightly asymmetric – there are apparently more vertices displaced from the interaction point in the jet flight direction than opposite to it. This suggests that those vertices correspond to the secondary decay points, as it is expected that a decaying heavy hadron will approximately follow the jet flight direction.

4.1.4 b Tag definition. Having reconstructed a jet vertex, the next step of the analysis was to define a b tag. Our basic requirement is that a tagged jet should have its vertex significantly displaced from the production point.

In order to quantify this statement assume that measured positions of the interaction point and jet vertex are given by $\mathbf{x}_{\mathrm{IP}}$ and $\mathbf{x}_{\mathrm{v}}$, with error matrices $\hat{\sigma}_{\mathrm{IP}}$ and $\hat{\sigma}_{\mathrm{v}}$ respectively. Assume further that the true jet vertex coincides with the true production point (i.e. no secondary decay vertex has been tagged). One can find the most probable coordinates of that true production point by minimising the quantity

$$\chi^2 = (\mathbf{x}-\mathbf{x}_{\mathrm{IP}})(\hat{\sigma}_{\mathrm{IP}})^{-1}(\mathbf{x}-\mathbf{x}_{\mathrm{IP}})^{\mathrm{T}} + (\mathbf{x}-\mathbf{x}_{\mathrm{v}})(\hat{\sigma}_{\mathrm{v}})^{-1}(\mathbf{x}-\mathbf{x}_{\mathrm{v}})^{\mathrm{T}}. \quad (22)$$

The minimum value of the above χ^2 (further called separation S) offers a good measure of the relative distance between the two points and has been used as a basic quantity defining a b tag. Figure 6 shows, as a result of a Monte Carlo simulation, the number of accepted events as a function of the separation cut, separately for different primary quark flavours. The b quark events start to dominate the accepted sample already at separa-

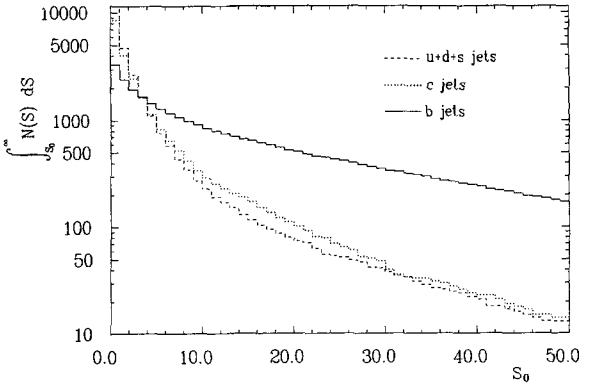

Fig. 6. The number of Monte Carlo jets with successful vertex fit remaining after the separation cut as a function of the cut; $S = \chi^2$

tion of about 7, and the purity of the sample grows quickly with increasing separation cut. It is interesting to note that the charm decay vertices are strongly reduced in the tagged sample, although the decay distances of charmed hadrons produced are close to those of the B hadrons. The main reason is the lower mass of the charmed hadrons, which causes their decay products to have a small opening angle in the detector. Some of the charm decay vertex candidates are removed by pre-fit cuts, and those surviving have on average larger reconstruction errors along the flight direction, and thus smaller separation.

An additional suppression of the background can be achieved by exploiting the fact that the decaying B hadron flight path is expected to follow approximately the event sphericity axis. A cut on the reconstructed vertex flight direction (i.e. angle ε between the jet axis and the line from the interaction point to the vertex) removes many spurious tags, which have their directions more randomly distributed. The Monte Carlo suggested the cut $\varepsilon < 23°$ as reducing the non-b background by more than 50%, still keeping more than 90% of the separated b vertices (the exact numbers depend somewhat on the separation cut).

4.1.5 The tagged sample purity. At this point of the analysis samples of various b content and number of events can be selected by varying the separation cut. The remaining problem is however to measure the purity of the resulting sample.

We decided to use the data themseves to estimate the b purity. To do this one can exploit the fact that both jets in an event are analysed completely independently. The main source of correlations in the tag probabilities between the two jets is the initiating quark flavour. Knowing the fractions of different quark flavours in the initial sample and counting the events with one and both jets tagged it is possible with few additional assumptions (that the tag probabilities for u, d and s initiating quarks are the same and that the ratio of the charm to light quark tag probabilities is as given by the Monte Carlo) to estimate the number of b production events in the tagged sample.

In the case of the asymmetry analysis a separation cut $S > 4.5$ has been used. It selected 979 tagged events, of which 33 had double tags. The b event content of this sample has been estimated to

$$P = 59 \pm 6 \pm 3\% \tag{23}$$

using as input the fractions of u, d, s, c and b events in the starting sample, the ration of uds/c tagging propability from Monte Carlo, and the number of single and double tag events given above. The value has been corrected for some residual correlations between the jets, caused by geometry (the polar and azimuthal angles of the two jets are by definition always opposite to each other) and by initial sample biasing by event selection criteria. The first error is statistical, dominated by the number of the doubly tagged events, and the other is systematic, coming from uncertainties in the initial sample quark content and correction estimation. The primary charm contribution to the sample has been estimated to be 21%.

This purity value has been checked by Monte Carlo simulation (which estimated 53% purity) and by the lepton methods described above (63%) – in agreement with the double tag value.

4.2 The quark charge determination

The lifetime tagging method does not give any hint about the charge of the primary b quark (i.e. does not distinguish between quarks and antiquarks). In order to measure the asymmetry we need some method to make this distinction.

We have decided to use the weighted jet charge idea of Field and Feynman [7]. The method envisages computing the quantity called the 'jet charge' defined by

$$q_{\text{jet}} = \sum_{\text{tracks}} q_i \left(\frac{p_i}{p_{\text{beam}}} \right)^{\gamma} \tag{24}$$

where the sum extends over all the tracks belonging to a jet, defined usually as a collection of particles moving in the same direction with respect to some axis. γ is some arbitrary parameter chosen to optimize the method. The jet charges of two opposite jets are then compared to each other, and the jet with higher charge is assigned positive primary quark charge. This method has been used to measure the asymmetry in flavour unseparated events [24].

In order to find and maximise the probability of correct primary quark charge assignment, a Monte Carlo simulation has been done. Two different Monte Carlo programs with different fragmentation schemes have been used to estimate the systematic errors: QCDFF with independent jet fragmentation and LUND with string fragmentation. An event has been divided in two jets by a plane perpendicular to the event sphericity axis. All tracks passing the standard TASSO quality cryteria have been used.

The inventors of the method [7] proposed originally using the parameter $\gamma = 0.5$ for best reconstruction of the quark charge. This choice has indeed been used by most analyses of this kind. In this analysis it has been found that for samples strongly enriched in b quarks $\gamma = 1.0$ gives possibly better results (both Monte Carlos agreed in this point). Table 5 shows the probabilities of correct charge reconstruction for various quark flavours in the two models, calculated from all events that passed the detector simulation.

To check for possible differences between the simulation and the data the distributions of some directly comparable quantities have been made and compared between the data and both models. As an example Fig. 7 shows the distribution of the higher jet charge. The models are in reasonable agreement with the data.

Table 5. Probability of a correct quark charge estimate for different primary flavours, as predicted by two Monte Carlo models

Quark	Model			
	QCDFF ($\gamma=0.5$)	LUND 6.3 ($\gamma=0.5$)	QCDFF ($\gamma=1$)	LUND 6.3 ($\gamma=1$)
u	0.7416 ± 0.0034	0.6817 ± 0.0037	0.7233 ± 0.0035	0.6749 ± 0.0037
d	0.6571 ± 0.0075	0.6087 ± 0.0078	0.6351 ± 0.0076	0.5991 ± 0.0078
s	0.6630 ± 0.0076	0.6110 ± 0.0078	0.6540 ± 0.0076	0.6072 ± 0.0078
c	0.6338 ± 0.0037	0.6445 ± 0.0037	0.5646 ± 0.0038	0.5989 ± 0.0038
b	0.6985 ± 0.0067	0.7157 ± 0.0055	0.7160 ± 0.0065	0.7162 ± 0.0067
average	0.6834 ± 0.0022	0.6587 ± 0.0022	0.6506 ± 0.0022	0.6383 ± 0.0023

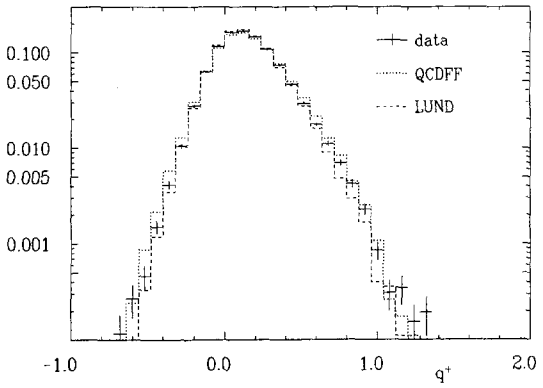

Fig. 7. The distribution of the higher of the two jet charges in an event. Data compared with two Monte Carlo models. The jet charge was calculated using $\gamma=1$

4.3 *The asymmetry measurement*

The asymmetry measurement was performed by measuring the negative jet flight direction with respect to the incoming electron. The event sphericity axis has been used as an approximation of the primary quark flight direction. A maximum likelihood fit to the form $N\cdot(1+\cos^2\theta+\frac{8}{3}\cdot A(q)\cdot\cos\theta)$ gave:

$$A(q)=-0.030\pm0.035. \tag{25}$$

In order to extract the b asymmetry from this number the contributions from non-b background have to be subtracted and the effect of finite charge reconstruction probability taken into account. The background of lighter quark events has been subtracted statistically, assuming the standard model values for the asymmetries, the c quark content of 21%, light quark ratios $u{:}d{:}s$ equal 4:1:1 and values from Table 5 for the charge estimate probabilities. The effect of a finite probability of correct charge reconstruction (p) on the measured asymmetry is to multiply the true value by a factor $(2p-1)$

$$A^{\text{meas}}=(2p-1)\cdot A^{\text{true}}. \tag{26}$$

The b quark asymmetry extracted from the data after these corrections is

$$A_b(q)=-0.14\pm0.14\pm0.04 \tag{27}$$

where the second error is the quadratic sum of systematic error contributions listed in Table 6.

5 Results

5.1 *Effect of the $B^0\bar{B}^0$ mixing*

A significant $B^0\bar{B}^0$ mixing has been observed by the ARGUS, CLEO and UA1 collaborations [25, 28]. We calculate the correction of the b quark asymmetry following [26]. We assume that we have only B mesons with u, d and s quark content. The fractions are expected to be equal to the production ratios of u, d and s quarks from the colour field of 1:1:0.4. This leads to the fractions $f_u=f_d=0.42$ and $f_s=0.16$. The mixing parameters may be defined as:

$$\chi_d=\frac{\Gamma(B_d^0\to\bar{B}_d^0\to\bar{X})}{\Gamma(B_d^0\to X \text{ or } \bar{X})}, \tag{28}$$

$$\chi_s=\frac{\Gamma(B_s^0\to\bar{B}_s^0\to\bar{X})}{\Gamma(B_s^0\to X \text{ or } \bar{X})}. \tag{29}$$

If we combine the results from ARGUS and CLEO we get $\chi_d=0.164\pm0.039$. The mixing parameter χ_s is ex-

Table 6. Contributions to the systematic error on A_b

Source	Contribution
b Content of the tagged sample	±0.025
Flavour composition of the background events	±0.020
Model dependencies of the charge identification probabilities for light flavours	±0.011
Error on the probability of charge identification in the b events	±0.005
Errors on the predicted asymmetries of the light flavours	±0.005

pected to be in the range $\chi_s = 0.47 \pm 0.03$ [27] which is in good agreement with the UA1 measurement. If we use that value we get an average mixing parameter of:

$$\chi = f_d \cdot \chi_d + f_s \cdot \chi_s = 0.144 \pm 0.022 \tag{30}$$

which is related to the ratio of the corrected b quark asymmetry to the measured b quark asymmetry

$$\frac{A_b^{\mathrm{cor}}(e)}{A_b(e)} = \frac{A_b^{\mathrm{cor}}(\mu)}{A_b(\mu)} = \frac{1}{1-2\cdot\chi} = 1.40 \pm 0.06. \tag{31}$$

It is less straightforward to determine the effect of mixing on the asymmetry measured from quark charge determination. The mixing affects the method by changing the probability of a correct jet charge assignment. The method uses however for the quark charge determination not only the tracks coming from B meson decay, but also those from primary fragmentation which are not affected by mixing and therefore the mixing effect is diminished. Moreover, the method compares the two jets in an event to get the quark charge, so even if a $B^0 \to \bar{B}^0$ transition occurs in one jet, the method does not necessarily change the charge assignment.

To determine the correction we used the same Monte Carlo sets as were used to estimate the charge reconstruction probability. The simulation of the mixing was performed by finding neutral B mesons in the fragmentation history record and reversing the charges of all their decay products with a probability given by the mixing parameters cited above. The probability of the correct quark charge assignment was then calculated again for the modified set. This method leads to a ratio of the corrected b quark asymmetry to the measured b quark asymmetry of

$$\frac{A_b^{\mathrm{cor}}(q)}{A_b(q)} = 1.18 \pm 0.05. \tag{32}$$

5.2 *Combined results*

We have measured the forward backward asymmetry $A = (F-B)/(F+B)$ in the reaction $e^+e^- \to b\bar{b}$ at centre of mass energies near 35 GeV with three different methods and on different event samples, yielding

$$A_b(e) = -0.20 \pm 0.11 \pm 0.04, \tag{33}$$

$$A_b(\mu) = -0.35 \pm 0.19 \pm 0.08, \tag{34}$$

$$A_b(q) = -0.14 \pm 0.14 \pm 0.04. \tag{35}$$

The results agree within the errors. If we combine the results of the measurements we get

$$\overline{A_b} = -0.21 \pm 0.08 \tag{36}$$

which is in good agreement with the results from other Experiments (see Table 1) as well as with our previous measurements. Taking the correction due to $B^0\bar{B}^0$ mixing into account leads to a corrected asymmetry of:

$$\overline{A_b^{\mathrm{cor}}} = -0.28 \pm 0.11. \tag{37}$$

6 Comparison with theory and conclusions

The differential cross section for the production of a fermion-antifermion pair in the e^+e^- annihilation can be expressed in lowest electroweak order, taking into account the fermion mass, as

$$\frac{d\sigma_{f\bar{f}}}{d\Omega} = \frac{d\sigma(e^+e^- \to f\bar{f})}{d\Omega}$$
$$= \frac{\alpha^2}{4\cdot s}\cdot[A\cdot(1+\cos^2\Theta_f) + B\cdot\cos\Theta_f + C\cdot\sin^2\Theta_f] \tag{38}$$

with coefficients A, B, C given in [34]. By integrating the cross section one finds

$$A_f = \frac{\int_0^1 \frac{d\sigma_{f\bar{f}}}{d\Omega}\,d(\cos\theta) - \int_{-1}^0 \frac{d\sigma_{f\bar{f}}}{d\Omega}\,d(\cos\theta)}{\int_{-1}^1 \frac{d\sigma_{f\bar{f}}}{d\Omega}\,d(\cos\theta)} = \frac{3}{8}\cdot\frac{B}{A+C/2}. \tag{39}$$

For numerical calculations of the b quark asymmetry we use $M_Z = 91.1\,\mathrm{GeV/c^2}$ [29], $\Gamma_Z = 2.6\,\mathrm{GeV/c^2}$, $\sin^2\theta_W = 0.227 \pm 0.004$ [30] and $m_b = 5.3\,\mathrm{GeV/c^2}$ [31]. This leads to:

$$A_b^0 = -0.25. \tag{40}$$

The b mass has a 1.5% effect only. Corrections due to higher order QED and QCD (without weak effects) are calculated with the LUND Monte Carlo (see Sect. 2.2). This leads to:

$$A_b^{\mathrm{SM}} = -0.23 \pm 0.03 \tag{41}$$

where the error is purely statistical in origin, coming from the finite number of Monte Carlo events available. This can be compared with our experimental result

$$\overline{A_b^{\mathrm{cor}}} = -0.28 \pm 0.11. \tag{42}$$

The axial vector coupling constant of the b quark as calculated from the corrected asymmetry is

$$a_b = -1.2 \pm 0.5 \tag{43}$$

in agreement with the standard model value of

$$a_b^{\mathrm{SM}} = -1. \tag{44}$$

Acknowledgements. We gratefully acknowledge the efforts of the PETRA machine group for high luminosity running, and the DESY directorate for their support. Those of us from abroad wish to thank the DESY directorate for the hospitality extended to us while working at DESY.

References

1. TASSO Coll. R. Brandelik et al.: Phys. Lett. 113B (1982) 499; TASSO Coll. R. Brandelik et al.: Phys. Lett. 114B (1982) 65
2. TASSO Coll. R. Brandelik et al.: Phys. Lett. 83B (1979) 261; TASSO Coll. R. Brandelik et al.: Phys. Lett. 94B (1980) 437; TASSO Coll. R. Brandelik et al.: Phys. Lett. 108B (1982) 71;

TASSO Coll. M. Althoff et al.: Z. Phys. C – Particles and Fields 26 (1984) 337; TASSO Coll. M. Althoff et al.: Phys. Lett. 146B (1984) 443; TASSO Coll. W. Braunschweig et al.: Z. Phys. C – Particles and Fields 33 (1986) 13
3. TASSO Coll. M. Althoff et al.: Phys. Lett. 146B (1984) 443
4. P. Rehders: D.Phil. Thesis, Hamburg 1989
5. P. Hoyer et al.: Nucl. Phys. B161 (1979) 349; A. Ali et al.: DESY Report, T80-01 (1980)
6. F.A. Behrends, R. Kleiss: Nucl. Phys. B178 (1981) 141
7. R.D. Field, R.P. Feynman: Nucl. Phys. B136 (1978) 1
8. K. Fabricius et al.: Z. Phys. C – Particles and Fields 11 (1982) 315; TASSO Coll. M. Althoff et al.: Z. Phys. C – Particles and Fields 26 (1984) 157
9. R.L. Ford, W.R. Nelson: SLAC Report 210 (1978)
10. A. Grant: Nucl. Instrum. Methods 131 (1975) 167
11. C. Peterson et al.: Phys. Rev. D27 (1983) 105
12. T. Sjöstrand: Comput. Phys. Commun. 27 (1982) 243; T. Sjöstrand: Comput. Phys. Commun. 28 (1983) 229; T. Sjöstrand: Comput. Phys. Commun. 39 (1986) 347
13. TASSO Coll. R. Brandelik et al.: Phys. Lett. 177B (1982) 135; TASSO Coll. M. Althoff et al.: Z. Phys. C – Particles and Fields 26 (1984) 157; K. Genser, Ph.D. Thesis, Warsaw 1989; P. Burrows: D.Phil. Thesis, Oxford RAL-T-071 1988
14. R. Marshall: Z. Phys. C – Particles and Fields 26 (1984) 291
15. TASSO Coll. M. Althoff et al.: Z. Phys. C – Particles and Fields 22 (1984) 307
16. J.P. Leveille: Proceedings of the 2nd Moriond Workshop, Les Arcs – Savoie 1982
17. R. Marshall: RAL Report 84-003 1984
18. TASSO Coll. M. Althoff et al.: Z. Phys. C – Particles and Fields 22 (1984) 219
19. TASSO Coll. W. Braunschweig et al.: Z. Phys. C – Particles and Fields 42 (1989) 17
20. D.M. Binnie et al.: Nucl. Instrum. Methods 228 (1985) 267
21. J.M. Pawlak: D.Phil. Thesis, Warsaw 1989
22. A.J. Campbell, D.Phil. Thesis, Imperial College London 1983, RL-HEP/T/117
23. D.H. Saxon: Nucl. Instrum. Methods A234 (1985) 258
24. W.W. Ash et al. (MAC Coll.): Phys. Rev. Lett. 58 (1987) 1080; TASSO Coll. W. Braunschweig et al.: Z. Phys. C – Particles and Fields 41 (1988) 385; JADE Coll. T. Greenshaw et al.: Z. Phys. C – Particles and Fields 42 (1989) 1
25. ARGUS Coll. H. Albrecht et al.: Phys. Lett. 192B (1987) 245; CLEO Coll. M. Artuso et al.: Phys. Rev. Lett. 62 (1989) 2233
26. Sau Lan Wu: Proceedings of the 1987 International Symposium on Lepton and Photon Interactions at High Energy Physics, Hamburg 1987, page 39
27. G. Altarelli, P. Franzini: Z. Phys. C – Particles and Fields 37 (1988) 271
28. UA1 Coll. C. Albajar et al.: Phys. Lett. 186B (1987) 247
29. L3 Coll. B. Adeva et al.: Phys. Lett. 231 (1989) 509; ALEPH Coll. D. Decamp et al.: Phys. Lett. 231 (1989) 519; OPAL Coll. M.Z. Akrang et al.: Phys. Lett. 231 (1989) 530; DELPHI Coll. P. Aarnio et al.: Phys. Lett. 231 (1989) 539; MARK II Coll. G.S. Abrams et al.: Phys. Rev. Lett. 63 (1989) 724; CDF Coll. F. Abe et al.: Phys. Rev. Lett. 63 (1989) 720
30. Review by D. Haidt: Nucl. Phys. B (Proc. Suppl.) 13 (1990) 3 and EPS Conf. Madrid 1989
31. H. Fritzsch: Phys. Lett. B166 (1986) 423
32. TPC Coll. H. Aihara et al.: Phys. Rev. D31 (1985) 2719; TPC Coll. H. Aihara et al.: Z. Phys. C – Particles and Fields 27 (1985) 39; CELLO Coll. H.J. Behrend et al.: Z. Phys. C – Particles and Fields 47 (1990) 333; JADE Coll. W. Bartel et al.: Phys. Lett. 146B (1984) 437; JADE Coll. E. Elsen et al.: Z. Phys. C – Particles and Fields 46 (1990) 349; Mark J Coll. B. Adeva et al.: Phys. Rep. 109 (1984) 133; TASSO Coll. M. Althoff et al.: Phys. Lett. 146B (1984) 443; TASSO Coll. M. Althoff et al.: Z. Phys. C – Particles and Fields 22 (1984) 219; MAC Coll. H.R. Band et al.: Phys. Lett. 218B (1989) 369; AMY Coll. H. Sagawa et al.: Phys. Rev. Lett. 63 (1989) 2341
33. CELLO Coll. H.J. Behrend et al.: Z. Phys. C – Particles and Fields 47 (1990) 333; JADE Coll. F. Ould-Saada et al.: Z. Phys. C – Particles and Fields 44 (1989) 567; Mark J Coll. B. Adeva et al.: Phys. Rep. 109 (1984) 133; TASSO Coll. W. Braunschweig et al.: Z. Phys. C – Particles and Fields 44 (1989) 365; HRS Coll. P. Baringer et al.: Phys. Lett. B206 (1988) 551
34. H.-U. Martyn: DESY 89-121; R. Marshall: Z. Phys. C – Particles and Fields 43 (1989) 607